HHS Public Access

Author manuscript

Eur J Med Chem. Author manuscript; available in PMC 2019 January 01.

Published in final edited form as:

Eur J Med Chem. 2018 January 01; 143: 1428–1435. doi:10.1016/j.ejmech.2017.10.038.

Development of Noviomimetics that Modulate Molecular Chaperones and Manifest Neuroprotective Effects

Leah K. Forsberg[†], **Mercy Anyika**[†], **Zhenyuan You**[‡], **Sean Emery**[‡], **Mason McMullen**[‡], **Rick T. Dobrowsky**[‡], and **Brian S. J. Blagg**[*,$]

[†]Department of Medicinal Chemistry, 1251 Wescoe Hall Drive, Malott 4070, The University of Kansas, Lawrence, Kansas 66045-7563

[‡]Department of Pharmacology and Toxicology Department, The University of Kansas, Lawrence, Kansas 66045, United States

[$]Department of Chemistry and Biochemistry, The University of Notre Dame, Notre Dame, Indiana 46556, United States

Abstract

Heat shock protein 90 (Hsp90) is a chaperone under investigation for the treatment of cancer and neurodegenerative diseases. Neuroprotective Hsp90 C-terminal inhibitors derived from novobiocin (novologues) include KU-32 and KU-596. These novologues modulate molecular chaperones and result in an induction of Heat Shock Protein 70 (Hsp70). “Noviomimetics” replace the synthetically complex noviose sugar with a simple cyclohexyl moiety to maintain biological efficacy as compared to novologues KU-596 and KU-32. In this study, we further explore the development of noviomimetics and evaluate their efficacy using a luciferase refolding assay, immunoblot analysis, a c-jun assay, and an assay measuring mitochondrial bioenergetics. These new noviomimetics were designed and synthesized and were found to induce Hsp70 and result in improved biological activity. Noviomimetics **39e** and **40a** were found to potently induce Hsp70 and in very promising effects in cellular assays.

Graphical abstract

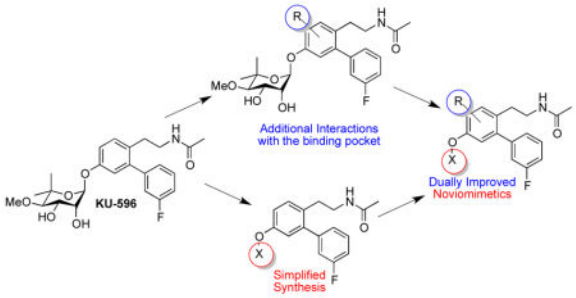

[*]Author to whom correspondence should be addressed. Phone: (574) 631-6877. bblagg@nd.edu.

Keywords

Molecular Chaperones; Heat Shock Protein 90; Heat Shock Protein 70; Novologues; Noviomimetics; Neurodegeneration

Introduction

Molecular chaperones represent promising therapeutic targets for both cancer and neurodegenerative diseases.[1–4] The 90kDa Heat Shock Protein 90 (Hsp90) is a molecular chaperone that is responsible for the folding and maturation of more than 300 client protein substrates.[5] Hsp90 modulates client protein substrates associated with all 10 hallmarks of cancer, supporting that inhibition of this chaperone may be useful for the treatment of cancer.[6–8] However, Hsp90 is also a target for neurodegenerative diseases since molecular chaperones can refold denatured proteins and resolubilize protein aggregates.[3, 9–14] The N-terminus of Hsp90 contains an ATP-binding site, and ATP hydrolysis provides the requisite energy needed to fold client protein substrates.[15–16] Currently, there are six N-terminal inhibitors undergoing clinical evaluation for the potential treatment of cancer.[17–18] Unfortunately, inhibition of the N-terminus and subsequent client protein degradation also leads to induction of the heat shock response (HSR), which results in the overexpression of the heat shock proteins, Hsp27, Hsp40, Hsp70 and Hsp90. [19–21] In contrast to N-terminal inhibitors, C-terminal inhibitors can segregate client protein degradation from induction of the pro-survival heat shock response.[22]

The DNA gyrase inhibitor, novobiocin (**1**), was the first Hsp90 C-terminal inhibitor discovered.[23] Through extensive structure-activity relationships, the natural product was modified to exhibit anti-proliferative activity.[24–26] Continued development of the potential cancer therapeutics led to the identification of cytotoxic replacements of the noviose sugar,[27–29] which improved inhibitor synthesis, as well as identification of new cores that target Hsp90, which could be used instead of the coumarin core.[30–33] These cytotoxic compounds provide an excellent platform for the treatment of cancer, as these analogs induce the degradation of Hsp90-client proteins, which in cancer cells leads to the disruption of multiple oncogenic pathways.[2]

Structure-activity relationship studies previously identified KU-32 (**2**) as an efficacious neuroprotective agent in cellular models of Alzheimer's disease.[34–35] Modulation of Hsp90 by **2** results in the induction of Hsp70 levels, which can refold denatured proteins, decrease the levels of abnormal proteins, and prevent protein aggregation, which can ultimately alleviate the phenotypes associated with many neurodegenerative diseases.[36] Subsequent studies demonstrated that **2** reversed clinical symptoms of Diabetic Peripheral Neuropathy (DPN) in vivo and protected against neuronal glucotoxicity.[37–39] A homology model of the Hsp90 C-terminus was then utilized to design a second generation of analogues, termed novologues (novobiocin analogues), which exchanged the coumarin core of **2** with a biphenyl ring system, and ultimately produced **3** (Figure 1A: Previous studies).[40–41] Although **3** exhibits promising activity and is undergoing pre-clinical evaluation, modeling studies with **3** identified unexplored regions within the C-terminal binding site that may

improve its activity, which ultimately led to the identification of noviomimetics (a non-noviosylated compound) **4**.[42] Preliminary studies with **4** confirmed that these noviomimetics maintained the desired biological activity of **3**, but are more synthetically desirable due to removal of the complex noviose sugar.[42–46] As a result, a new library of novologues and noviomimetics were designed in which modifications were incorporated to gain additional interactions with the binding pocket (Figure 1A: Current Study). Several compounds obtained from this third generation library exhibit improved activity when compared to **3** and **4** as described herein.

Results and Discussion

A homology model of the Hsp90 C-terminus was utilized for the design of new novologues, and demonstrated the potential for a binding pocket adjacent to the noviose sugar in **3** as illustrated in Figure 1B. During prior studies wherein replacements of the noviose sugar were explored, **4** was identified as a simplified novologue that exhibited similar biological activity to **3**.[42] As shown in Figure 1B, the noviose surrogate projects into this previously unexplored binding pocket and therefore modifications to the benzyl ring on **4** were explored to identify improved modulators. Modifications at the *ortho-* position were investigated to determine whether hydrogen bonding interactions could be established with GLU537, GLN682, or nearby amino acids (Figure 1B). Substituents at the *meta-* and *para-* positions were explored to identify potential hydrophobic interactions at this location. In addition, modification to the central ring of **3** was sought to determine whether hydrogen bond donors or acceptors could interact with the peptide backbone (Figure 1B). The substituents chosen for these studies included both electronic and steric functionalities to establish preliminary structure-activity relationships.

Synthesis of phenol **9**[41] (Scheme 1A) commenced by benzyl protection of 2,4-dihydroxybenaldehyde, **5**. The resulting benzyl ether was converted to trifluoromethanesulfonate **6**, in the presence of N-Phenyl bis-trifluoromethane sulfonimide and potassium carbonate using microwave conditions.[47] A subsequent Suzuki coupling reaction with commercially available 3-fluorophenyl boronic acid was employed to generate the biaryl ring system found in **7**, which was then subjected to a Henry reaction, followed by simultaneous reduction of both the nitro and olefin functionalities with lithium aluminum hydride to yield amine **8**. Acylation of **8** was followed by cleavage of the benzyl ether under hydrogenolysis conditions to afford the phenol, **9**.

Compounds **14b–u** were obtained via an S_N2 substitution reaction between phenol **9** and the toluenesulfonates of the corresponding sugar surrogates (Scheme 1B).[48] Compound **18** was obtained by a Mitsunobu reaction between phenol **9** and the corresponding sugar mimic. Novologue **18** was then subjected to an osmium tetroxide catalyzed dihydroxylation to obtain the corresponding diol, **19** (Scheme 1C).

Synthesis of each derivative that contained a modified core began via different starting materials. Synthesis of compound **26** commenced by reduction of commercially available 2,4-dihydroxybenzaldehyde with sodium cyanoborohydride in the presence of HCl (Scheme 2A).[49] The resulting methylbenzene was formylated to obtain 2,4-dihydroxy-5-

methylbenzaldehyde, which was then benzyl protected to produce **20**.[50] Compound **20** was then subjected to the same conditions utilized to produce phenol **9**, and ultimately yielded phenol **25** (Scheme 2A). The noviose sugar was synthesized using a previously reported procedure.[43–46] The protected sugar was activated (**24**)[51] and then coupled with **25** using Schmidt conditions.[52] Solvolysis of the carbonate with triethylamine and methanol provided the final product, **26**. Synthesis of **29** and **31** began by formylation of phloroglucinol, followed by benzyl protection of 2,4,6-trihydroxybenzaldehyde using potassium carbonate and benzyl bromide to yield **27**. To achieve the final product **29**, **27** was subjected to dimethyl sulfide in water and acetone to yield the methyl ether, **28** (Scheme 2B).[53] This key intermediate was then subjected to the conditions previously described in Scheme 2B, to obtain **29**.

Compound **31** was obtained by the treatment of **27** with chloromethyl methyl ether chloride to produce the mono-protected phenol **30** (Scheme 2C),[54–55] which was then subjected to the conditions previously described to give **31**. Synthesis of compound **34** began by selective benzylation of 2,3,4-trihydroxybenzyaldehyde, which was then subjected to chloromethyl methyl ether formation to produce intermediate **33**. Similarly, compound **33** was subjected to conditions previously described to achieve the free phenol, which was then coupled with the trichloroacetamide of noviose carbonate and upon solvolysis, gave **34**. Synthesis of compound **37** was initiated by subjecting 2-nitrobenzene 1,3-diol to a Duff reaction.[56] The resulting product was then benzyl protected to yield compound **36**, which was modified according to the conditions highlighted in Scheme 2E to obtain the final product, **37**.

We have previously shown that the cytoprotective activity manifested by KU-32 and KU-596 requires Hsp70 induction. Therefore, upon construction of the library of noviomimetics, we evaluated Hsp70 induction via a luciferase reporter assay (Figure 2A).

As shown in Figure 2A, 14e induced the most robust Hsp70 levels for the new noviomimetics. Generally, the noviomimetics with substitutions at the *para*- and *ortho*-positions appear to manifest increased Hsp70 levels. Whereas, substitutions at the *meta*-position appear detrimental, as less Hsp70 induction occurred, **14i–k**. The *para*-substituted noviomimetics showed greater induction of Hsp70 than the corresponding *ortho*-noviomimetics (**14c, f–h**). Generally, electron-withdrawing groups at the *para*- position produced the most robust Hsp70 induction, followed by electron donating groups at the *ortho*- position. Similarly, **19** is a *para*-substituted noviomimetic that contains a cyclohexyl *cis*-diol and also yielded good activation of the luciferase promoter. The *cis*-diol of **19**, mimics the noviose sugar more than the unsubstituted cyclohexane ring, which may explain its enhanced activity.

Immunoblot analyses were then performed to further examine the effect of select noviomimetics on Hsp70 protein expression. Compounds **4**, **14b**, **14g**, and **14h** all resulted in induction of Hsp70. Consistent with the induction of luciferase activity via the Hsp70 promoter; *ortho*- and *para*-substituted noviomimetics induced Hsp70 protein expression as evidenced by **14b**, **14g, 14h, 18,** and **19** (Figure 2B). Additionally *meta*-substituted noviomimetics resulted in a decreased induction of Hsp70 when compared to similarly substituted *ortho*- and *para*-noviomimetics, as evidenced by **14q** and **14o**. Dually modified,

14r, demonstrated the least amount of Hsp70 induction, suggesting that the binding pocket does not tolerate modifications at both the *ortho*- and *para*-position. Surprisingly, **18** and **19** were less effective in the immunoblot assay, despite a robust induction of luciferase activity. The remaining *para*- and *ortho*- substituted compounds were similarly effective when comparing activity between the luciferase assay and the immunoblot assay. Due to the promising biological activity in both assays, 4 noviomimetic side chains (**14b–e)** were selected for further investigation.

Comparison studies between the noviomimetic side chains and the original KU-32 coumarin scaffold were carried out to further elucidate positive neuroprotective effects. Additionally, comparison studies were conducted to verify which core could provide the greatest Hsp70 induction. The coumarin containing noviomimetics (**46**–**49**, supporting information, Figure SI) were synthesized with selected noviomimetic side chains. Using the luciferase reporter assay, the phenol for each scaffold and noviomimetics **46–49,** were evaluated (Supporting Information, Figure S1). Scaffolds **9** and **45** did not contain any sugar moiety/surrogate and were found to be inactive. Noviomimetics containing the KU-32 coumarin scaffold exhibited less activity than their biaryl counterparts (Figure SI).

The decrease in Hsp70 induction by **46**–**49** could result from the rigid coumarin core. The biphenyl core offers enhanced flexibility that is not available with the coumarin core, which may allow for improved interactions within the binding pocket. Increasing flexibility may also be important due to the increase in length of the noviomimetic side chain compared to noviose sugar. Substitutions on the central ring were evaluated using immunoblot analysis to observe Hsp70 level and to support improved interactions with the binding pocket. The novologues were analyzed at varying concentrations (30, 100, 300, 1000, and 3000nM) as shown in Figure 3A.

Novologues containing substituted central rings produced improved Hsp70 induction as compared to **3** (Figure 3A). Novologues **26** and **34** resulted in the largest induction of Hsp70. It is possible that the methyl substituent present in **26**, overlays in three-dimensional space with **2**, and reinstates interactions that are lost when moving from the coumarin core to the biphenyl ring system. Furthermore, the data supports the importance of having a hydrophobic substitution on the central core, as **26** resulted in the greatest induction of Hsp70. In continuation, the novologues containing central core substituents were coupled with selected noviomimetics (**13a**–**e**). These noviomimetics were synthesized as described in Scheme 2 and then analyzed via immunoblot analysis to evaluate Hsp70 induction.

As shown in Figure 3B, noviomimetics **39a**, **39d**, **40a**, and **41d** resulted in the greatest Hsp70 induction. Collectively, all noviomimetics with a methoxy group at the 3-position (**39a**–**e**) resulted in increased Hsp70 levels compared to noviomimetics with other central ring modifications. Interestingly, none of the methyl containing noviomimetics (**38a**–**d**) resulted in improved Hsp70 induction, which was unexpected since **26** resulted in the greatest induction of all of the central ring modifications. It is likely that switching from the noviose sugar to a noviomimetic alters binding, and ultimately leads to a decrease in Hsp70 levels. Noviomimetics containing a phenol on the central ring were similarly active when located at the 3- or 6- positions (**40a–e** and **41a–e**), and only the noviomimetic side chain

seemed to impact induction of Hsp70. Noviomimetic side chains **a** and **d** appear to produce the most robust induction of Hsp70, regardless of the central ring modification, and therefore provide desired neuroprotective activity.

Validation of Hsp90 Inhibition via the c-Jun Assay and Mitochondrial Bioenergetic (mtBE) Assessment

Further assessment of the neuroprotective activity manifested by select noviomimetics was carried out after confirmation of the desired cytoprotective response and induction of Hsp70 levels. As such, noviomimetics **29**, **31**, **39d**, **39e**, **40a**, **40b**, and **41d** were selected for further biological evaluation in an assay to evaluate c-jun levels.

Hsp70 regulates c-jun levels by increasing its degradation via the proteasome (Figure 4).[57] Therefore, induction of Hsp70 via noviomimetics results in the degradation of c-jun. The assay was carried out by treating 50B11 cells with serum free media for 24 hours, resulting in cell cycle arrest and a decrease in the expression of c-jun. The cells were then treated with vehicle or 1.0 μM of the indicated noviomimetic, and c-jun was induced by placing the cells in medium containing 10% FBS for 2 hours. The protein was harvested and c-Jun levels were evaluated.

All of the selected noviomimetics decreased c-Jun levels when compared to the untreated control (Figure 4). Importantly, most noviomimetics exhibited improved activity when compared to **3**, and a few had improved activity as compared to **4**. The general trend of the data illustrates that noviomimetics with a free phenol at the 3-position were more effective than noviomimetics with a methoxy at the 3-position. Excitingly, noviomimetic **40a** resulted in the greatest reduction in c-Jun levels. Reduction of c-Jun levels by all noviomimetics suggests that the mechanism of action occurs via induction of Hsp70.

Prior work indicated that the neuroprotective efficacy manifested by **2** to improve the symptoms of diabetic peripheral neuropathy was associated with an increase in mitochondrial respiration. To determine whether the increase in Hsp70 expression correlated with mitochondrial respiration, 50B11 cells were treated with various noviomimetics for 24 hours (Figure 5). Mitochondrial respiration was then measured in intact cells using an XF96 extracellular flux analyzer, which provides concurrent measures of mitochondrial oxygen consumption rates (OCR) and extracellular acidification rates (ECAR) as an indication of glycolytic activity. A variety of noviomimetics were selected to examine this correlation between Hsp70 expression and mitochondrial respiration effects on mitochondrial respiration.

Hydrogenperoxide can induce cellular apoptosis through mitochondrial dysfunction. 0.5mM hydrogen peroxide can cause mitochondrial bioenergetics (mtBE) loss, indicated by largely decreased response to FCCP. **3** and **4** effectively improved mtBE, however the dually modified noviomimetics resulted in decreased maximal respiratory capacity (Figure 5). Surprisingly, noviomimetic **39e** was the most effective at increasing the MRC, even though it was not as efficacious in the c-jun assay as the other noviomimetics. The different results

obtained from these two assays are due to each assay relying upon a different cellular mechanism for the analyzed biological result.

Conclusion

In conclusion, a library of novologues was designed with the goal of replacing the synthetically complex noviose sugar with a simplified sugar surrogates. The current work supports that noviomimetics can successfully retain the ability to increase Hsp70 expression and mitochondrial function, two mechanistic features that are associated with the neuroprotective efficacy of both biaryl-based novologues such as **4** and novobiocin-based compounds such as **3**. Noviomimetic **40a** exhibited promising effects in the c-Jun assay, while **39e** was effective at increasing the MRC. Thus, noviomimetics may serve as a new series of synthetically simplistic, neuroprotective compounds for treating various neurodegenerative diseases.

Supplementary Material

Refer to Web version on PubMed Central for supplementary material.

Acknowledgments

This work was supported by grants [CA109265] to BSJB; [DK095911] to RTD and [NS075311] to BSJB and RTD from The National Institutes of Health.

References

1. Khandelwal A, Crowley VM, Blagg BSJ. Natural Product Inspired N-Terminal Hsp90 Inhibitors: From Bench to Bedside? Medicinal Research Reviews. 2016; 36(1):92–118. [PubMed: 26010985]
2. Hall JA, Forsberg LK, Blagg BSJ. Alternative Approaches to Hsp90 Modulation for the Treatment of Cancer. Future Medicinal Chemistry. 2014; 6(14):1587–1605. [PubMed: 25367392]
3. Zhao, H., Michaelis, ML., Blagg, BSJ. Hsp90 Modulation for the Treatment of Alzheimer's Disease. In: Elias, KM., Mary, LM., editors. Advances in Pharmacology. Vol. 64. Academic Press; 2012. p. 1-25.
4. Zhao H, Mary LM, Blagg BSJ. Hsp90 Modulation for the Treatment of Alzheimer's Disease. Advances in Pharmacology. 2012; 64
5. Karagoz GE, Rudiger SGD. Hsp90 interaction with clients. Trends in biochemical sciences. 2015; 40(2):117–25. [PubMed: 25579468]
6. Miyata Y, Nakamoto H, Neckers L. The Therapeutic Target Hsp90 and Cancer Hallmarks. Current Pharmaceutical Design. 2013; 19(3):347–365. [PubMed: 22920906]
7. Hanahan D, Weinberg RA. The Hallmarks of Cancer. Cell. 2000; 100:57–70. [PubMed: 10647931]
8. Hanahan D, Weinberg RA. Hallmarks of cancer: the next generation. Cell. 2011; 144(5):646–74. [PubMed: 21376230]
9. Pratt WB, Morishima Y, Gestwicki JE, Lieberman AP, Osawa Y. A model in which heat shock protein 90 targets protein-folding clefts: Rationale for a new approach to neuroprotective treatment of protein folding diseases. Experimental Biology and Medicine (Maywood). 2014; 239(11):1405–13.
10. Ebrahimi-Fakhari D, Saidi L-J, Wahlster L. Molecular chaperones and protein folding as therapeutic targets in Parkinson's disease and other synucleinopathies. Acta Neuropathologica Communications. 2013; 1(1):79. [PubMed: 24314025]

11. Hoozemans JJ, Haastert ESv, Nijholt DA, Rozemuller AJ, Scheper W. Activation of the unfolded protein response is an early event in Alzheimer's and Parkinson's disease. Neurodegenerative Disease. 2012; 10
12. Blair LJ, Sabbagh JJ, Dickey CA. Targeting Hsp90 and its co-chaperones to treat Alzheimer's disease. Expert Opinion Therapeutic Targets. 2014; 18(10)
13. Ghosh S, Liu Y, Garg G, Anyika M, McPherson NT, Ma J, Dobrowsky RT, Blagg BSJ. Diverging Novobiocin Anti-Cancer Activity from Neuroprotective Activity through Modification of the Amide Tail. ACS Medicinal Chemistry Letters. 2016; 7(8):813–8. [PubMed: 27563408]
14. Saibil H. Chaperone Machines for Protein Folding, Unfolding and Disaggregation. Nature reviews. Cancer. 2013; 14(10):630–42.
15. Schopf FH, Biebl MM, Buchner J. The HSP90 chaperone machinery. Nature Reviews Molecular Cell Biology. 2017; 18(6):345–360. [PubMed: 28429788]
16. Röhl A, Rohrber J, Buchner J. The Chaperone Hsp90: Changing Partners for Demanding Clients. Trends in biochemical sciences. 2013; 38(5):253–62. [PubMed: 23507089]
17. Neckers L, Trepel JB. Stressing the development of small molecules targeting HSP90. Clinical cancer research: an official journal of the American Association for Cancer Research. 2014; 20(2): 275–7. [PubMed: 24166908]
18. Neckers L, Workman P. Hsp90 Molecular Chaperone Inhibitors: Are We There Yet? Clinical cancer research: an official journal of the American Association for Cancer Research. 2012; 18(1): 64–76. [PubMed: 22215907]
19. Bharadwaj S, Ali A, Ovsenek N. Multiple Components of the Hsp90 Chaperone Complex Function in Regulation of Heat Shock Factor 1 in Vivo. Molecular and Cellular Biology. 1999; 19(12): 8033–8041. [PubMed: 10567529]
20. Morimoto RI. Regulation of the heat shock transcriptional response: cross talk between a family of heat shock factors, molecular chaperones, and negative regulators. Genes Dev. 1998; 12
21. Whitesell L, Bagatell R, Falsey R. The Stress Response; Implications for the Clinical Development of Hsp90 Inhibitors. Current Cancer Drug Targets. 2003; 3(5):349–358. [PubMed: 14529386]
22. Isaacs J, Whitesell L. Advances in Cancer Research. 2016; 129
23. Marcu MG, Schulte TW, Neckers L. Novobiocin and Related Coumarins and Depletion of Heat Shock Protein 90-Dependent Signaling Proteins. Journal of the National Cancer Institute. 2000; 92(3):242–248. [PubMed: 10655441]
24. Burlison JA, Avila C, Vielhauer G, Lubbers DJ, Holzbeierlein J, Blagg BSJ. Development of Novobiocin Analogues that Manifest Anti-Proliferative Activity Against Several Cancer Cell Lines. Journal of Organic Chemistry. 2008; 73:2130–2137. [PubMed: 18293999]
25. Donnelly AC, Mays JR, Burlinson JA, Nelson JT, Vielhauer G, Holzbeierlein J, Blagg BSJ. The Design, Synthesis and Evaluation of Coumarin Ring Derivatives of the Novobiocin Scaffold that Exhibit Antiproliferative Activity. Journal of Organic Chemistry. 2008; 73:8901–8920. [PubMed: 18939877]
26. Zhao H, Donnelly AC, Kusuma BR, Brandt GEL, Brown D, Rajewski RA, Vielhauer G, Holzbeierlein J, Cohen MS, Blagg BSJ. Engineering an Antibiotic to Fight Cancer: Optimization of the Novobiocin Scaffold to Produce Anti-Proliferative Agents. Journal of medicinal chemistry. 2011; 54(11):3839–53. [PubMed: 21553822]
27. Donnelly AC, Zhao H, Kusuma BR, Blagg BSJ. Cytotoxic Sugar Analogues of an Optimized Novobiocin Scaffold. Medicinal Chemistry Communication. 2010; 1(2):165–170.
28. Zhao H, Kusuma BR, Blagg BSJ. Synthesis and Evaluation of Noviose Replacements on Novobiocin that Manifest Anti-proliferative Activity. ACS Medicinal Chemistry Letters. 2010; 1(7):311–315. [PubMed: 21904660]
29. Zhao H, Blagg BSJ. Novobiocin Analogues with Second-Generation Noviose Surrogates. Bioorganic & Medicinal Chemistry Letters. 2013; 23(2):552–7. [PubMed: 23234644]
30. Kusuma BR, Khandelwal A, Gu W, Brown D, Liu W, Vielhauer G, Holzbeierlein J, Blagg BSJ. Synthesis and Biological Evaluation of Coumarin Replacements of Novobiocin as Hsp90 Inhibitors. Bioorganic & medicinal chemistry. 2014; 22(4):1441–1449. [PubMed: 24461493]
31. Zhao H, Moroni E, Colombo G, Blagg BSJ. Identification of a New Scaffold for Hsp90 C-Terminal Inhibition. ACS Medicinal Chemistry Letters. 2014; 5(1):84–88. [PubMed: 24900777]

32. Byrd KM, Subramanian C, Sanchez J, Motiwala HF, Liu W, Cohen MS, Holzbeierlein J, Blagg BSJ. Synthesis and Biological Evaluation of Novobiocin Core Analogues as Hsp90 Inhibitors. Chemistry- A European Journal. 2016; 22(20):6921–31.
33. Forsberg LK, Garg G, Zhao H, Blagg BSJ. Development of Phenyl Cyclohexylcarboxamides as a Novel Class of Hsp90 C-terminal Inhibitors. Chemistry – A European Journal. n/a-n/a.
34. Ansar S, Burlison JA, Hadden MK, Yu XM, Desino KE, Bean J, Neckers L, Audus KL, Michaelis ML, Blagg BSJ. A non-toxic Hsp90 inhibitor protects neurons from Abeta-induced toxicity. Bioorganic & Medicinal Chemistry Letters. 2007; 17(7):1984–90. [PubMed: 17276679]
35. Lu Y, Ansar S, Michaelis ML, Blagg BSJ. Neuroprotective activity and evaluation of Hsp90 inhibitors in an immortalized neuronal cell line. Bioorganic & medicinal chemistry. 2009; 17(4): 1709–15. [PubMed: 19138859]
36. Pratt WB, Gestwicki JE, Osawa Y, Lieberman AP. Targeting Hsp90/Hsp70-based protein quality control for treatment of adult onset neurodegenerative diseases. Annual Review Pharmacology Toxicology. 2015; 55:353–71.
37. Urban MJ, Li C, Yu C, Lu Y, Krise JM, McIntosh MP, Rajewski RA, Blagg BSJ, Dobrowsky RT. Inhibiting heat-shock protein 90 reverses sensory hypoalgesia in diabetic mice. ASN neuro. 2010; 2(4):e00040. [PubMed: 20711301]
38. Dobrowsky RT. Targeting the Diabetic Chaperome to Improve Peripheral Neuropathy. Current Diabetes Reports. 2016; 16(8):71. [PubMed: 27318486]
39. Ma J, Pan P, Anyika M, Blagg BSJ, Dobrowsky RT. Modulating Molecular Chaperones Improves Mitochondrial Bioenergetics and Decreases the Inflammatory Transcriptome in Diabetic Sensory Neurons. ACS Chemical Neuroscience. 2015; 6(9):1637–48. [PubMed: 26161583]
40. Matts RL, Dixit A, Peterson LB, Sun L, Voruganti S, Kalyanaraman P, Hartson SD, Verkhivker GM, Blagg BSJ. Elucidation of the Hsp90 C-Terminal Inhibitor Binding Site. ACS chemical biology. 2011; 6(8):800–7. [PubMed: 21548602]
41. Kusuma BR, Zhang L, Sundstrom T, Peterson LB, Dobrowsky RT, Blagg BSJ. Synthesis and evaluation of novologues as C-terminal Hsp90 inhibitors with cytoprotective activity against sensory neuron glucotoxicity. Journal of medicinal chemistry. 2012; 55(12):5797–812. [PubMed: 22702513]
42. Anyika M, McMullen M, Forsberg LK, Dobrowsky RT, Blagg BSJ. Development of Noviomimetics as C-Terminal Hsp90 Inhibitors. ACS Medicinal Chemistry Letters. 2016; 7(1): 67–71. [PubMed: 26819668]
43. Matsushima Y, Kino J. Novel Concise Synthesis of (±)-Noviose and l-(+)-Noviose by Palladium-Catalyzed Epoxide Opening. Synthesis. 2011; 2011(08):1290–1294.
44. Reddy DS, Srinivas G, Rajesh BM, Kannan M, Rajale TV, Iqbal J. Enantiospecific synthesis of (−)-d-noviose from (−)-pantolactone. Tetrahedron Letters. 2006; 47(36):6373–6375.
45. Rajesh BM, Shinde MV, Kannan M, Srinivas G, Iqbal J, Reddy DS. Enantiodivergent routes to (+) and (−)-novioses from (−)-pantolactone. RSC Advances. 2013; 3(43):20291.
46. Schmidt B, Hauke S. Metathesis-Based De Novo Synthesis of Noviose. European Journal of Organic Chemistry. 2014; 2014(9):1951–1960.
47. Bengtson A, Hallberg A, Larhed M. Fast Synthesis of Aryl Triflates with Controlled MIcrowave Heating. Organic Letters. 2002; 4(7):1231–1233. [PubMed: 11922826]
48. Blagg, BSJ., Dobrowsky, RT., Anyika, M. Google Patents. 2016. Biphenyl amides with modified ether groups as hsp90 inhibitors and hsp70 inducers.
49. Xie L, Takeuchi Y, Cosentino LM, Lee KH. Anti-AIDS Agents. 37. Synthesis and Structure-Activity Relationshps of (3′R,4′R)-(+)-cis-Khellactone Derivatives as Novel Potent Anti-HIV Agents. Journal of medicinal chemistry. 1999; 42:2662–2672. [PubMed: 10411486]
50. Ohsawa K, Yoshida M, Doi T. A direct and mild formylation method for substituted benzenes utilizing dichloromethyl methyl ether-silver trifluoromethanesulfonate. Journal of Organic Chemistry. 2013; 78(7):3438–44. [PubMed: 23477294]
51. Yu XM, Shen G, Blagg BSJ. Synthesis of (−)-Noviose from 2,3-O-Isopropylidene-D-erthyronolactol. Journal of Organic Chemistry. 2004; 69:7375–7378. [PubMed: 15471498]

52. Andrieux CP, Farriol M, Gallardo I, Marquet J. Thermodynamics and kinetics of homolytic cleavage of carbon-oxygen bonds in radical anions obtained by electrochemical reduction of alkyl aryl ethers. Journal of the Chemical Society, Perkin Transactions 2. 2002; (5):985–990.

53. Li CC, Xie ZX, Zhang YD, Chen JH, Yang Z. Total Synthesis of Wedelolactone. Journal of Organic Chemistry. 2003; 68:8500–8504. [PubMed: 14575477]

54. Kogen H, Toda N, Tago K, Marumoto S, Takami K, Ori M, Yamada N, Koyama K, Naruto S, Abe K, Yamazaki R, Hara T, Aoyagi A, Abe Y, Kaneko T. Design and Synthesis of Dual Inhibitors of Acetylcholinesterase and Serotonin Transporter Targeting Potential Agents for Alzheimer's Disease. Organic Letters. 2002; 4(20):3359–3362. [PubMed: 12323018]

55. Toda, Narihiro, Tago, Keiko, Marumoto, Shinji, Takami, Kazuko, Ori, Mayuko, Yamada, Naho, Koyama, Kazuo, Naruto, Shunji, Abe, Kazumi, Yamazaki, Reina, Hara, Takao, Aoyagi, Atsushi, Abe, Yasuyuki, Kaneko, Tsugio, Kogen, Hiroshi. A Conformational Restriction Approach to the Development of Dual Inhibitors of Acetylcholinesterase and Serotonin Transporter as Potential Agents for Alzheimer's Disease. Bioorganic & medicinal chemistry. 2003; 11(20):4389–4415. [PubMed: 13129577]

56. Garg G, Zhao H, Blagg BSJ. Design, synthesis, and biological evaluation of ring-constrained novobiocin analogues as hsp90 C-terminal inhibitors. ACS Medicinal Chemistry Letters. 2015; 6(2):204–9. [PubMed: 25699150]

57. Li C, Ma J, Zhao H, Blagg BSJ, Dobrowsky RT. Induction of heat shock protein 70 (Hsp70) prevents neuregulin-induced demyelination by enhancing the proteasomal clearance of c-Jun. ASN neuro. 2012; 4(7):e00102. [PubMed: 23240583]

Highlights

- Treatment of 50B11 cells with Noviomimetics induced Hsp70 levels
- Noviomimetics decreased c-JUN levels in 50B11 cells
- Noviomimetic treatment improved mitochondrial bioenergetics

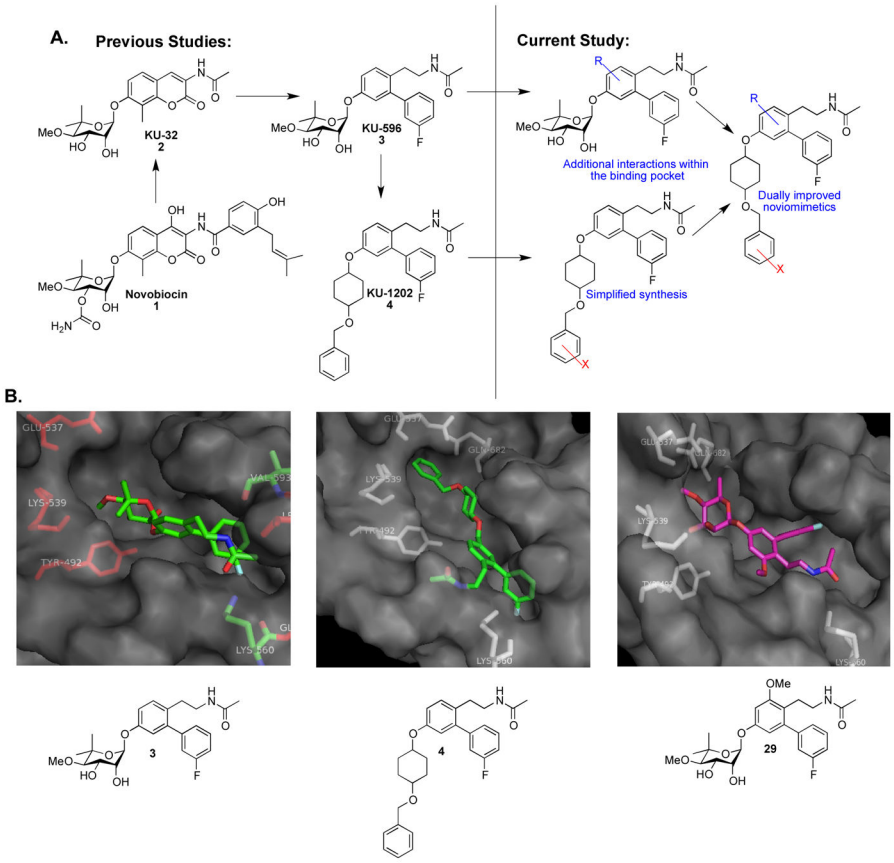

Figure 1.

A). A summary of prior and current studies presented herein. B). Compounds **3** (KU-596), **4**, and **29** docked to Hsp90 C-terminal homology model.

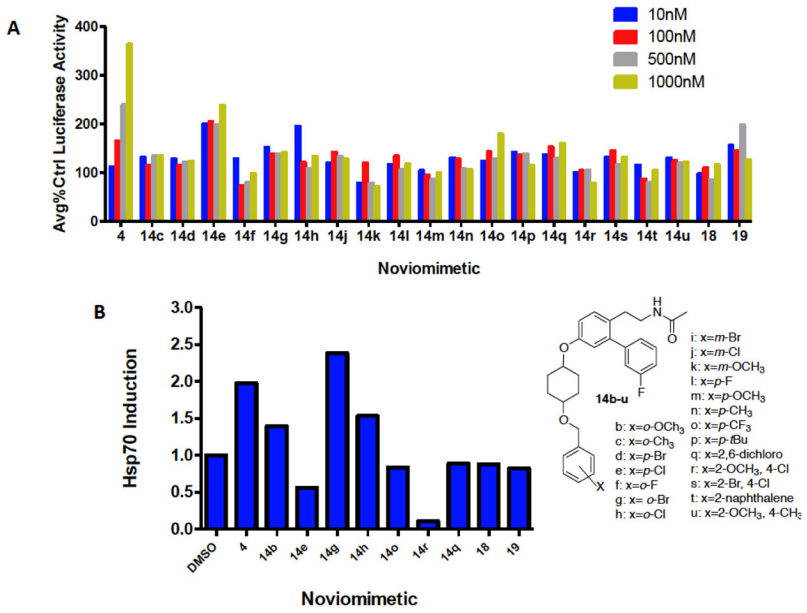

Figure 2.

A). Evaluation of Hsp70 induction via noviomimetics in a Luciferase Reporter Assay. Results are mean ±SEM. (n = 3–9). **c**: x = *o*-CH_3; **d**: x = *p*-Br; **e**: x = *p*-Cl; **f**: x = *o*-F; **g**: x = *o*-Br; **h**: x = *o*-Cl; **j**: x = *m*-Cl; **k**: x = *m*-OCH_3, **l**: x = *p*-F; **m**: x = *p*-OCH_3; **n**: x = *p*-CH_3; **o**: x = *p*-CF_3; **p**: x = *p*-*t*Bu; **q**: x = 2, 6-dichloro; **r**: x = 2-OCH_3, 4-Cl; **s**: x = 2-Br, 4-Cl; **t**: x = 2-naphthalene; **u**: x = 2-OCH_3, 4-CH_3. B). Induction of Hsp70 protein expression by select noviomimetics. 50B11 cells were treated for 24hr with 1 μM of the indicated Novologues or DMSO, the negative control. Immunoblot analysis was performed and densitometry was used to report fold induction of Hsp70. A representative blot is located in Supplemental Figure 2.

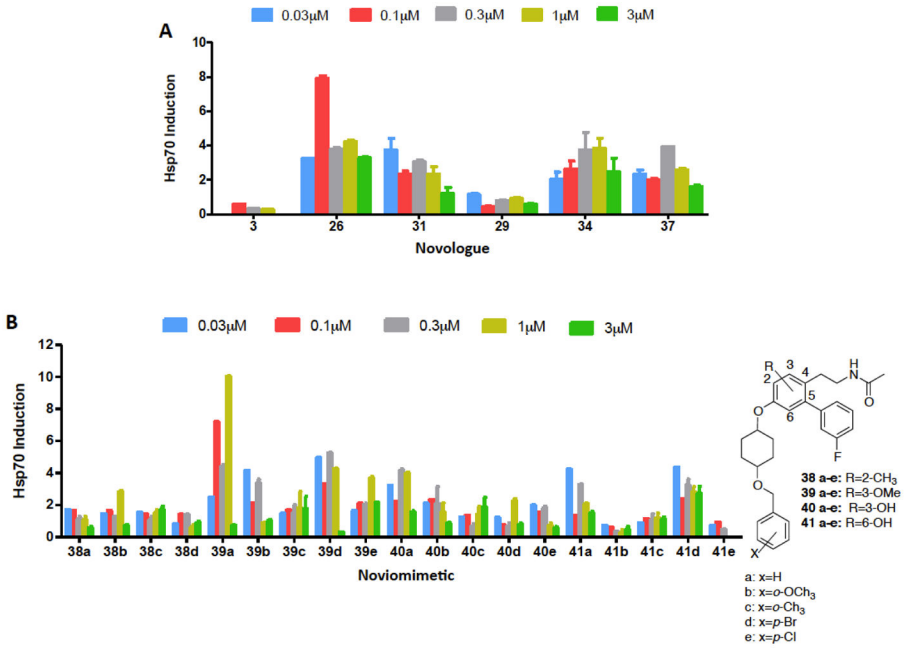

Figure 3.

A). Immunoblot analysis of Hsp70 induction of novologues in nontransfected 50B11 cells. 50B11 cells were treated for 24hr with the indicated Novologues or DMSO as the negative control. Immunoblot analysis was performed and densitometry was used to report fold induction of Hsp70. Results are mean ±SEM. (n >2). B). Immunoblot analysis of Hsp70 induction of dually modified noviomimetics in nontransfected 50B11 cells. 50B11 cells were treated for 24hr with the indicated Noviomimetic or DMSO as the negative control. Immunoblot analysis was performed and densitometry was used to report fold induction of Hsp70. A representative immunoblot can be found in supplemental figure 3. Results are mean ±SEM. (n >2).

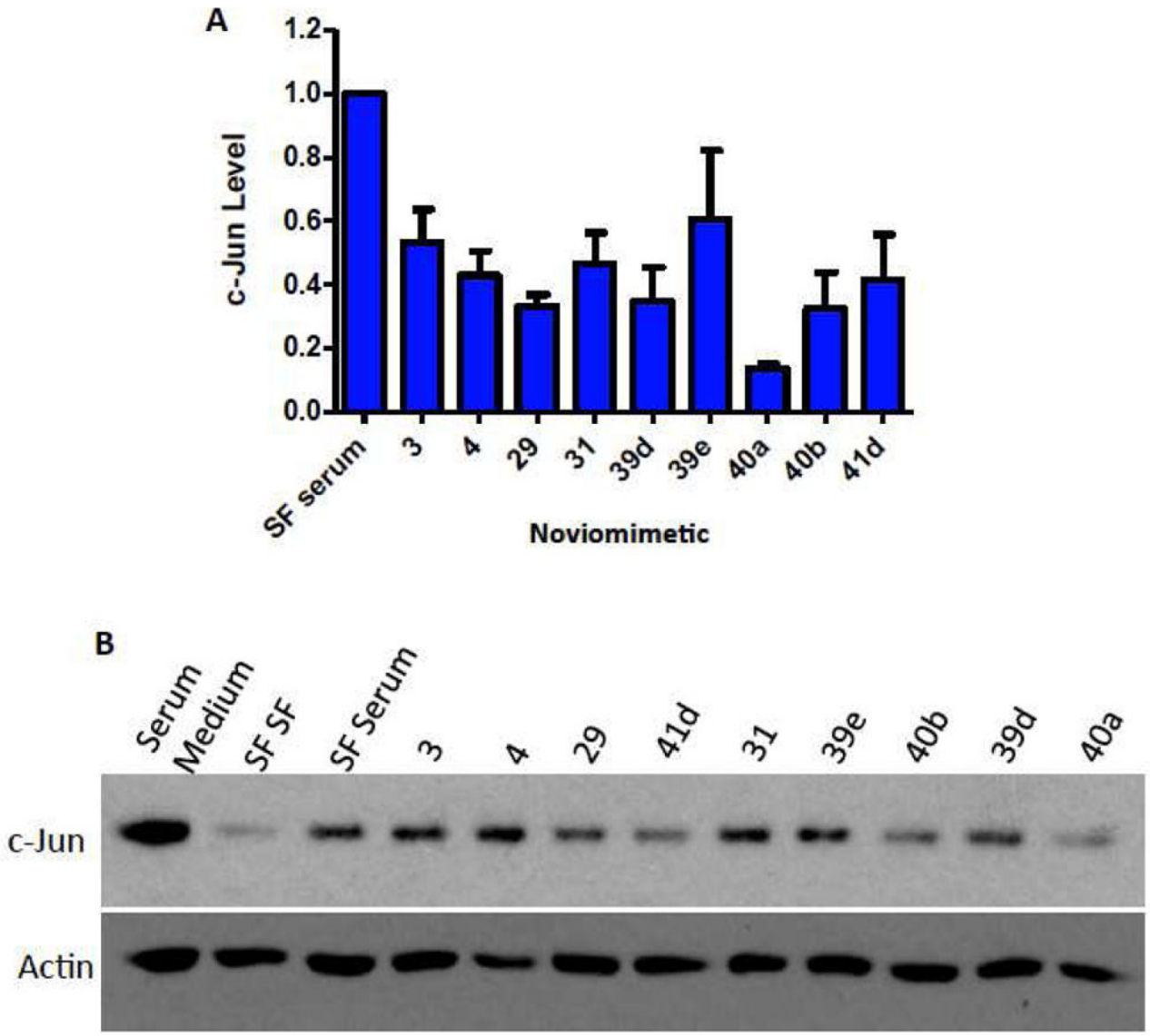

Figure 4.

c-Jun levels in 50B11 cells upon treatment with 1.0 μM of noviomimetic for 24 hours. C-Jun was upregulated by placing the cells in 10% serum containing media for 2 hours. The cell lysates were then collected for immunoblot analysis. A). c-Jun levels in response to Noviomimetic treatment, normalized to SF Serum. B). Representative immunoblot of c-Jun and Actin (control) for the tested noviomimetics. Immunoblot analysis was performed and densitometry was used to report fold induction of c-Jun. Results are mean ±SEM. (n >2).

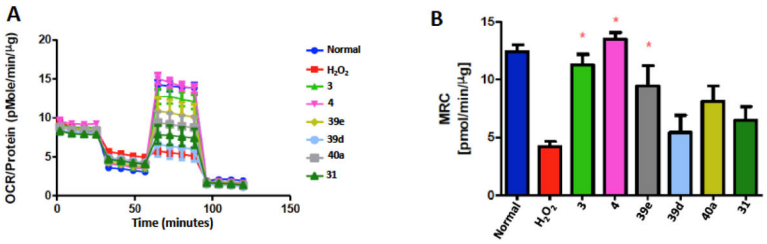

Figure 5.

Compound 19 enhances mitochondrial function. A). 50B11 cells were seeded into the 96 well plates, maintained in high glucose DMEM supplemented with 10% fetal bovine serum. After 12 hours, 50B11 cells were changed into high glucose DMEM medium with 1% FBS, treated together with 1.0 μM **3**, **4**, **39d**, **39e**, **40a**, **31**. After 24 hr, the cells were stressed with 0.5mM H_2O_2 for 2hr. H_2O_2 can largely inhibit 50B11 mitochondrial bioenergetics, indicated by largely decreased response to FCCP. 1μM **3**,**4** and **39e** can significantly increase cellular Maximal Respiratory Capacity (MRC) of oxidative stress. 50B11 cells were treated for 16 hr with DMSO, **3**, **4**, **31**, **39e**, **39d**, **40a**. B). Bar graph representation of data acquired in A, * $p<0.05$ vs H_2O_2.

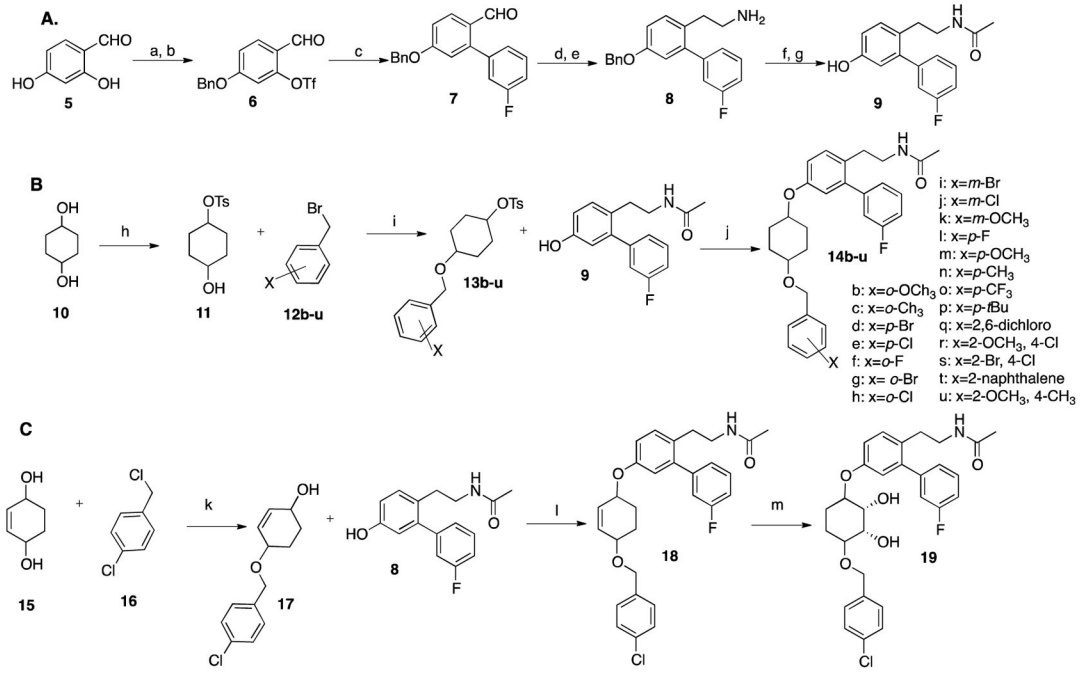

Scheme 1.

A). Synthesis of phenol **9**. Reaction conditions to make phenol **9**: *a.* BnBr, $NaHCO_3$, CH_3CN, 75%; *b.*$(CF_3CO)_2O$, Et_3N, DCM, 60%; *c.*3-fluoro-phenylboronic acid, $Pd(PPh_3)_4$, K_2CO_3, DMF, 90%; *d.* CH_3NO_2, NH_4OAc, 98%; *e.* $LiAlH_4$, THF, 30 min, *f.* Ac_2O, Et_3N, 72% over 2 steps, *g.* H_2, Pd/C, MeOH, 90%. B). Synthesis of Noviomimetics **14b–u**: *h.* TsCl, Pyridine, 0 °C-rt, on $CHCl_3$; *i.* NaH, Acetonitrile, rt, 16hr; *j.* K_2CO_3, DMF, 80°C, 2d, 55–80%; **b**: x = *o*-OCH_3; **c**: x = *o*-CH_3; **d**: x = *p*-Br; **e**: x = *p*-Cl; **f**: x = *o*-F; **g**: x = *o*-Br; **h**: x = *o*-Cl; **i**: x = *m*-Br; **j**: x = *m*-Cl; **k**: x = *m*-OCH_3, **l**: x = *p*-F; **m**: x = *p*-OCH_3; **n**: x = *p*-CH_3; **o**: x = *p*-CF_3; **p**: x = *p*-*t*Bu; **q**: x = 2, 6-dichloro; **r**: x = 2-OCH_3, 4-Cl; **s**: x = 2-Br, 4-Cl; **t**: x = 2-naphthalene; **u**: x = 2-OCH_3, 4-CH_3. C). Synthesis of compounds **18** and **19**: *k.* NaH, DMF, rt, on, 60%; *l.* PPh_3, DIAD, THF, rt, 3h, 58%; *m.* OsO_4, NMO, THF/H_2O, on, 83%.

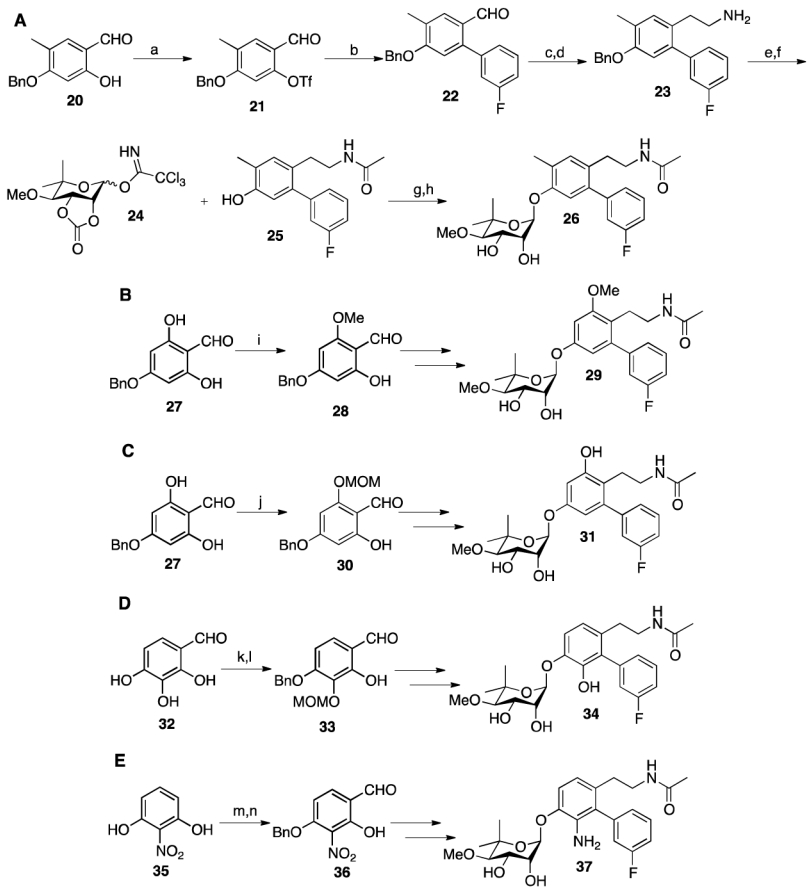

Scheme 2.

A). Synthesis of **26**. *a.* $(CF_3CO)_2O$, Et_3N, DCM, 60%; *b.* 3-fluoro-phenylboronic acid, $Pd(PPh_3)_4$, K_2CO_3, DMF, 90%; *c.* CH_3NO_2, NH_4OAc, 98%; *d.* $LiAlH_4$, THF, 30 min; *e.* Ac_2O, Et_3N, 72% over 2 steps; *f.* H_2, Pd/C, MeOH, 90%; *g.* BF_3OEt, DCM, 40%; *h.* Et_3N, MeOH, 85%. B). Synthesis of **29**: *i.* Me_2SO_4, K_2CO_3, H_2O/Acetone (1/1), 55%; C). Synthesis **31**: *j.* MOMCl, DIPA, DCM, 65%; D). Synthesis of **34**: *k.* $NaHCO_3$, BnBr, MeCN, 45%; *l.* MOMCl, DIPEA, DCM, 70%; E). Synthesis of **37**: *m.* Hexamethylenetetramine, Trifluoroacetic Acid, 25%; *n.* $NaHCO_3$, BnBr, KI, MeCN, 75%.